

## A submersible imaging-in-flow instrument to analyze nano- and microplankton: Imaging FlowCytobot

Robert J. Olson and Heidi M. Sosik

Biology Department, MS 32, Woods Hole Oceanographic Institution, Woods Hole, Massachusetts, USA

### Abstract

A fundamental understanding of the interaction between physical and biological factors that regulate plankton species composition requires, first of all, detailed and sustained observations. Only now is it becoming possible to acquire these types of observations, as we develop and deploy instruments that can continuously monitor individual organisms in the ocean. Our research group can measure and count the smallest phytoplankton cells using a submersible flow cytometer (FlowCytobot), in which optical properties of individual suspended cells are recorded as they pass through a focused laser beam. However, FlowCytobot cannot efficiently sample or identify the much larger cells (10 to >100  $\mu\text{m}$ ) that often dominate the plankton in coastal waters. Because these larger cells often have recognizable morphologies, we have developed a second submersible flow cytometer, with imaging capability and increased water sampling rate (typically, 5 mL seawater analyzed every 20 min), to characterize these nano- and microplankton. Like the original, Imaging FlowCytobot can operate unattended for months at a time; it obtains power from and communicates with a shore laboratory, so we can monitor results and modify sampling procedures when needed. Imaging FlowCytobot was successfully tested for 2 months in Woods Hole Harbor and is presently deployed alongside FlowCytobot at the Martha's Vineyard Coastal Observatory. These combined approaches will allow continuous long-term observations of plankton community structure over a wide range of cell sizes and types, and help to elucidate the processes and interactions that control the life cycles of individual species.

### Introduction

Several research planning groups have noted that time series sensors able to monitor plankton community structure, in addition to those measuring bulk properties such as chlorophyll, are needed to adequately investigate questions about coastal ocean ecosystems (SCOTS Steering Committee 2002; Daly et al. 2004; Jahnke et al. 2004). With the goal of better understanding how coastal plankton communities are regulated, we have begun a high-resolution, long-term plankton monitoring program at the Martha's Vineyard Coastal Observatory (MVCO) (Austin et al. 2000; Austin et al. 2002). FlowCytobot, a

submersible flow cytometer that uses fluorescence and light scattering signals from a laser beam to characterize the smallest phytoplankton cells (~1–10  $\mu\text{m}$ ) (Olson et al. 2003; Sosik et al. 2003), has been deployed at MVCO for most of the past 3 years. Other instruments, such as the Autonomous Vertically Profiling Plankton Observatory (Thwaites et al. 1998) are capable of monitoring plankton at the other end of the size spectrum (mainly zooplankton >100  $\mu\text{m}$ ). However, plankton in the size range 10 to 100  $\mu\text{m}$  are not well sampled by either of these instruments. This is a critical gap because phytoplankton in this size range, which includes many diatoms and dinoflagellates, can be especially important in coastal blooms, and microzooplankton, such as protozoa, are critical to the diets of many grazers including copepods and larval fish.

Nano- and microplanktonic organisms can be studied in the laboratory or on board ships with a commercially available imaging flow cytometer, the FlowCAM (Sieracki et al. 1998). Other submersible flow cytometers have been developed, such as the CytoSub (e.g., Cunningham et al. 2003), but to our knowledge none has the necessary resolution and field endurance for the ecological studies we wish to carry out. Therefore we developed our own submersible imaging flow cytometer, based on FlowCytobot.

### Acknowledgments

This research was supported by grants from NSF (Biocomplexity IDEA program and Ocean Technology and Interdisciplinary Coordination program; OCE-0119915 and OCE-0525700) and by funds from the Woods Hole Oceanographic Institution (Bigelow Chair, Ocean Life Institute, Coastal Ocean Institute, and Access to the Sea Fund). We are indebted to Alexi Shalapyonok for expert technical assistance, Tatiana Orlova (Institute of Marine Biology, Russian Academy of Sciences) for manual microscopic plankton analyses, Tom Hurst and Glenn McDonald for electrical and mechanical engineering support, and the Martha's Vineyard Coastal Observatory operations team, especially Janet Fredericks, for logistical support.

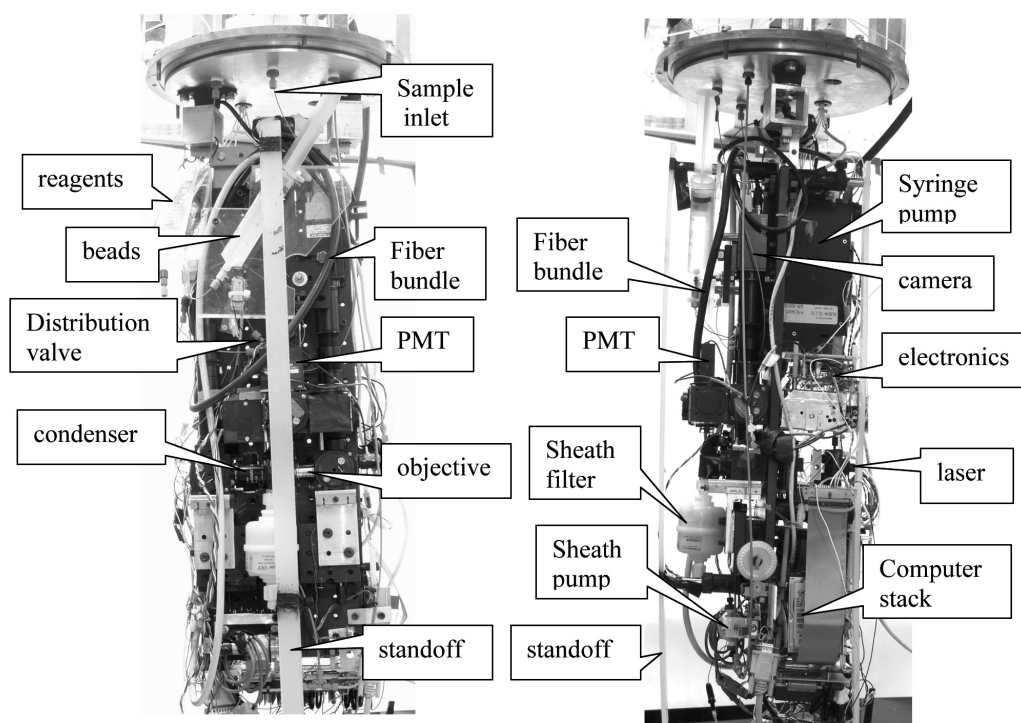


**Fig. 1.** Imaging FlowCytobot, removed from underwater housing. Three plastic standoffs prevent contact of the components and housing during installation. Left: front view, showing the “fluidics and optics” side of the optical breadboard. The flow cell (hidden by standoff) is located between the condenser and objective lenses. Right: side view; the optical breadboard is edge-on in the center, with fluidics/optics components mounted to the left and electronics to the right.

Imaging FlowCytobot uses a combination of video and flow cytometric technology to both capture images of organisms for identification and measure chlorophyll fluorescence associated with each image. Images can be automatically classified with software based on a support vector machine (Sosik and Olson 2007), and the measurements of chlorophyll fluorescence allow us to more efficiently analyze phytoplankton cells by triggering on chlorophyll-containing particles. Quantitation of chlorophyll fluorescence in large phytoplankton cells will also enable us to better interpret patterns in bulk chlorophyll data and to discriminate heterotrophic from phototrophic cells.

Imaging FlowCytobot’s design was intended to follow, as far as possible, that of the original FlowCytobot, because of that instrument’s history of reliability in field deployments. A seawater sample is injected into the center of a sheath flow of particle-free water; all the particles are thus confined to the center of the flow cell, which ensures that each particle is in focus as it passes through the optical system. An important feature of the design is that the sheath fluid is recycled through a filter cartridge, which removes sample particles after they have been analyzed. This feature allows for the efficient use of antifouling agents so the system can operate for months at a time without the need for maintenance or cleaning. The instrument is contained in a watertight

housing, and it operates continuously and autonomously under the direction of a computer whose programming can be modified by a remote operator. Programmable operations include data acquisition and transfer to shore, adjustment of sampling frequency and rate of injection, injection of internal standard beads, flushing the flow cell and/or sample tubing with detergent, backflushing the sample tubing to remove potential clogs, adding sodium azide to the sheath reservoir to prevent biofouling of the internal surfaces, and focusing the imaging objective lens.

### Methods and Procedures

*Mechanical/electrical*—Imaging FlowCytobot is constructed around an optical breadboard (20.32 by 60.96 cm) with mostly off-the-shelf components; the fluid-handling and electronic components are mounted on opposite sides of the breadboard (Fig. 1). The breadboard hangs from the instrument end cap, which seals to the watertight housing (30.48 cm inner diameter by 76.2 cm) via 2 nitrile o-rings and has external connections to an MVCO guest port for power and Ethernet communication with shore. Power is supplied as 36V DC (100 W). Communication (10 megabits s<sup>-1</sup>) between the instrument and the MVCO guest port are via category-5 cable, and between the guest port and the shore laboratory via optic fiber (Austin et al. 2000; Austin et al. 2002).

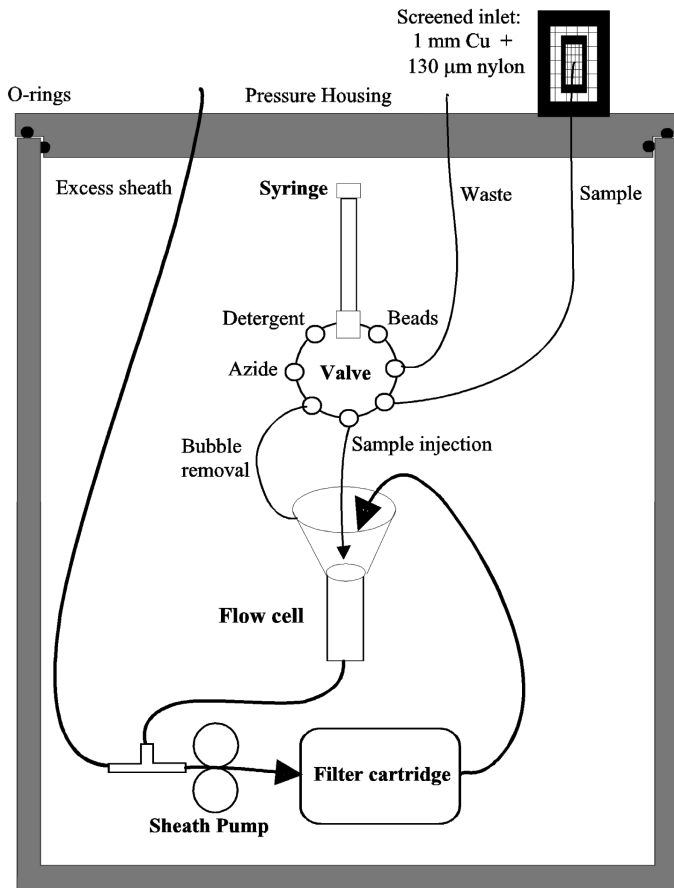


**Fig. 2.** Schema of fluidics system of Imaging FlowCytobot.

**Fluidics system**—Imaging FlowCytobot’s fluidics system (Fig. 2) is based on that of a conventional flow cytometer: hydrodynamic focusing of a seawater sample stream in a particle-free sheath flow carries cells in single file through a laser beam (and then through the camera’s field of view). The fluidics and sampling system is similar to that of the original FlowCytobot except that, to minimize problems due to settling of large particles, the syringe is mounted vertically rather than horizontally and the flow through the flow cell is downward rather than upward.

The sheath fluid, seawater forced through a pair of 0.2- $\mu\text{m}$  filter cartridges (Supor; Pall Corp.) by a gear pump (Micropump, Inc. Model 188 with PEEK gears), flows through a conical chamber to a quartz flow cell. The flow cell housing and sample injection tube is from a Becton Dickinson FACScan flow cytometer, but the flow cell is replaced by a custom cell with a wider channel (channel dimensions 860 by 180  $\mu\text{m}$ ; Hellma Cells, Inc.). Because the FACScan objective lens housing, which normally supports the plastic flow cell assembly, is not used here, an aluminum plate (3.175 mm thick) is bolted to the assembly.

A programmable syringe pump (Versapump 6 with 48,000-step resolution, using a 5-mL syringe with Special-K plunger; Kloehn, Inc.) is used to sample seawater through a 130- $\mu\text{m}$

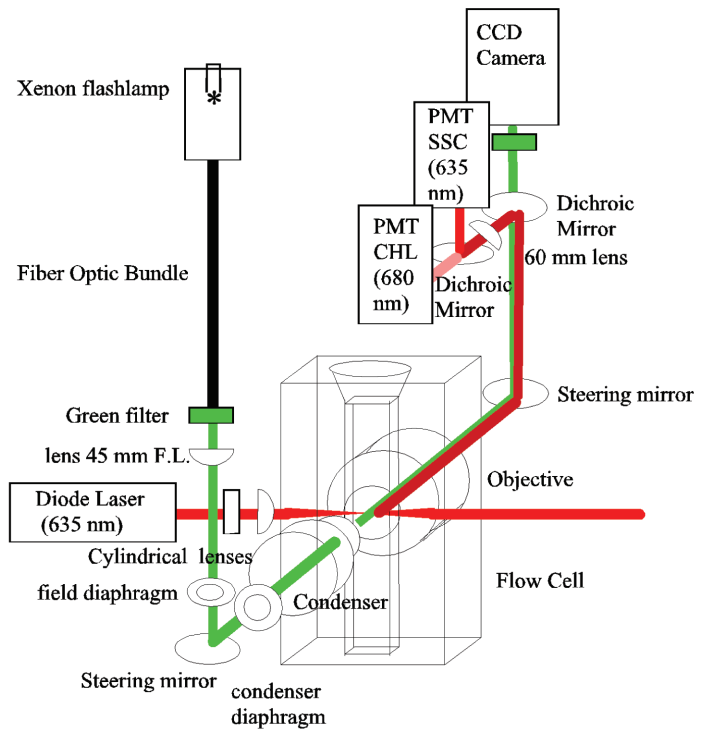


**Fig. 3.** Schema of optical layout of Imaging FlowCytobot.

Nitex screen (to prevent flow cell clogging), which is protected against biofouling by 1 mm copper mesh. The sample water is then injected through a stainless steel tube (1.651 mm OD, 0.8382 mm internal diameter; Small Parts, Inc.) into the center of the sheath flow in the cone above the flow cell. The tubing is of PEEK material (3.175 by 1.575 mm external and internal diameter for sheath tubes, 1.588 by 0.762 mm for others; Upchurch Scientific).

An 8-port ceramic distribution valve (Kloehn, Inc.) allows the syringe pump to carry out several functions in addition to seawater sampling. These include regular (~daily) addition of sodium azide to the sheath fluid (final concentration ~0.01%) to prevent biofouling, and regular (~daily) analyses of beads (20 or 9  $\mu\text{m}$  red-fluorescing beads; Duke Scientific, Inc.) as internal standards to monitor instrument performance. In addition, during bead analyses (~20 min  $\text{d}^{-1}$ ), the sample tubing (which is not protected from biofouling by contact with azide-containing sheath fluid) is treated with detergent (5% Contrad/1% Tergazyme mixture) to remove fouling. Finally, the syringe pump is used to prevent accumulation of air bubbles (from degassing of seawater) in the flow cell, which could disrupt the laminar flow pattern; before each sample is injected, sheath fluid is withdrawn (along with any air bubbles) through both the sample injection needle and the conical region above the flow cell, and discarded to waste. Azide solution, suspended beads, and detergent mixture are stored in 100-mL plastic bags with Luer fittings (Stedim Biosystems).

**Optical system**—Flow cytometric measurements are derived from a red diode laser (SPMT, 635 nm, 12 mW, Power Technologies, Inc.) focused to a horizontally elongated elliptical beam spot by cylindrical lenses (horizontal = 80 mm focal length, located 100 mm from the flow cell; vertical = 40 mm focal length, at 40 mm). Each particle passing through the laser beam scatters laser light, and chlorophyll-containing cells emit red (680 nm) fluorescence (Fig. 3). One of these signals (usually chlorophyll fluorescence) is chosen to trigger a xenon flash lamp (Hamamatsu L4633) when the signal exceeds a preset threshold; the resulting 1- $\mu$ s flashes of light are used to provide Kohler illumination of the flow cell. The green component of the light (isolated by a bandpass filter) is focused into a randomized fiber optic bundle (50  $\mu$ m fibers, 6.35 mm diameter; Stocker-Yale, Inc.). At the bundle exit, the light is collected by a lens, passes through a field iris, and is focused onto a condenser iris located approximately at the back focal plane of a 10 $\times$  objective lens (Zeiss CP-Achromat, numerical aperture [N.A.] 0.25), which is in turn focused on the flow cell. A second 10 $\times$  objective (Zeiss Epiplan, N.A. 0.2) collects the light from both flash lamp illumination (green) and laser (red, 635 nm scattered light and 680 nm chlorophyll fluorescence). Green and red wavelengths are separated by a dichroic mirror (590 nm short pass); green light continues to a monochrome CCD camera (UniqVision UP-1800DS-CL, 1380 by 1034 pixels), and red light is reflected to a second dichroic (635 LP), which directs scattered laser light and fluorescence to separate photomultiplier (PMT) modules (Hamamatsu HC120-05 modified for current-to-voltage conversion with time constant = 800 kHz; the PMT for laser scattering also incorporates DC restoration circuitry).

The optical path is folded by broadband dielectric mirrors (Thorlabs BB1-E02) on either side of the flow cell to conserve space. The flow cell assembly is fixed to the optical table, and the light source/condenser and objective/PMT/camera assemblies are each mounted on lockable translators (Newport Corp.) providing 3 degrees of freedom for adjustment. The objective focusing translator is remotely controllable (see Instrument Control below). Optical mounting hardware is from Thorlabs, Inc.

**Data acquisition and instrument control**—Imaging FlowCytobot is controlled by a PC-104plus computer (Kontron MOPS-LCD7, 700 MHz) running Windows XP (Microsoft Corp.). Remote operation is carried out via Virtual Networking Computing software (www.realvnc.com). The camera is configured and the syringe pump is programmed by software provided by the manufacturers; all other functions (control, image visualization, and data acquisition) are carried out by custom software written in Visual Basic 6 (Microsoft Corp.).

A custom electronics board amplifies and integrates light scattering and fluorescence signals, and also generates control pulses for timing purposes (Fig. 4). The signal from the triggering PMT (typically chlorophyll fluorescence) is split, with one part sent to a comparator circuit that produces a trigger pulse if the signal is larger than a preset threshold

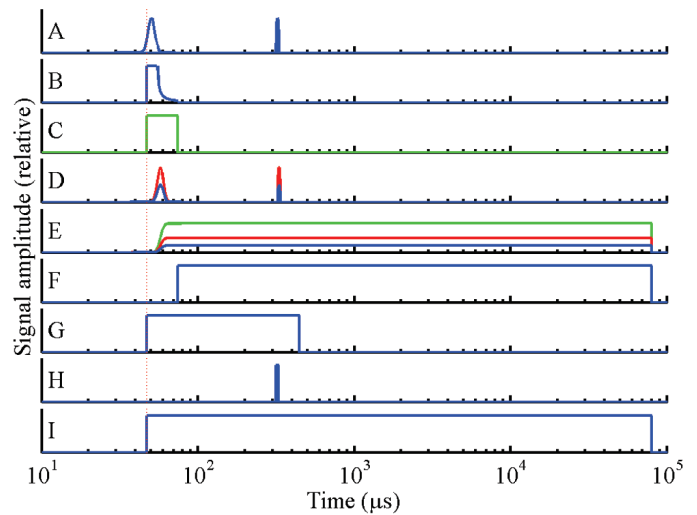


**Fig. 4.** Imaging FlowCytobot signals and controls. When a trigger signal (from the chlorophyll fluorescence PMT) exceeds a preset level (A), a comparator produces a logic signal (B); the decay of this signal is artificially slowed by a capacitor so that the integration window (C) does not miss signals from closely following cells, as for chain diatoms. The chlorophyll fluorescence and side scattering PMT signals, delayed by 7  $\mu$ s (D), are integrated and held (E), as is the logic signal itself (to provide an estimate of signal duration). At the end of the integration window, the held signals are digitized (F). The original signal also triggers the CCD camera (G) and a 270  $\mu$ s flash lamp timer (H) (note the flash lamp signals in A and D). The original signal also triggers a “reset” pulse (I) lasting 80 ms, during which time no other triggers can be detected. (In the case of large cells whose image processing requires >80 ms, this “dead” time is extended through software-mediated grounding of the trigger signal amplifier input and measured via a Visual Basic timer.)

level. The other part of the signal, and the signal from the other PMT, are delayed by 7  $\mu$ s (by delay modules from a Coulter Electronics EPICS 750 flow cytometer) and then split and sent to paired linear amplifiers with 25-fold different gains (to increase dynamic range) before integration (Burr-Brown AFC2101). The delay modules allow the pretrigger portions of the signals to be included in the integration. The end of the integration window is also determined by the comparator, with the provision that the signal remains below the comparator threshold for 20  $\mu$ s; this allows signals from loosely connected cells such as chain diatoms to be more accurately measured. Comparator output pulses are also integrated to provide an estimate of the duration of each signal. The PMT amplifier inputs are grounded by transistors during flash lamp operation to avoid baseline distortion by the very large signals from the flashes (Fig. 4A, D).

The trigger pulse is also sent to a frame grabber board (Matrox Meteor II CL) to begin image acquisition, and, after a delay of 270  $\mu$ s, to the flash lamp, which illuminates the flow cell for a 1- $\mu$ s exposure. Integration of light scattering and fluorescence signals is limited to 270  $\mu$ s to avoid contamination by light from the flash lamp, so integrated signals from cells or chains longer than  $\sim$ 600  $\mu$ m are minimum estimates.

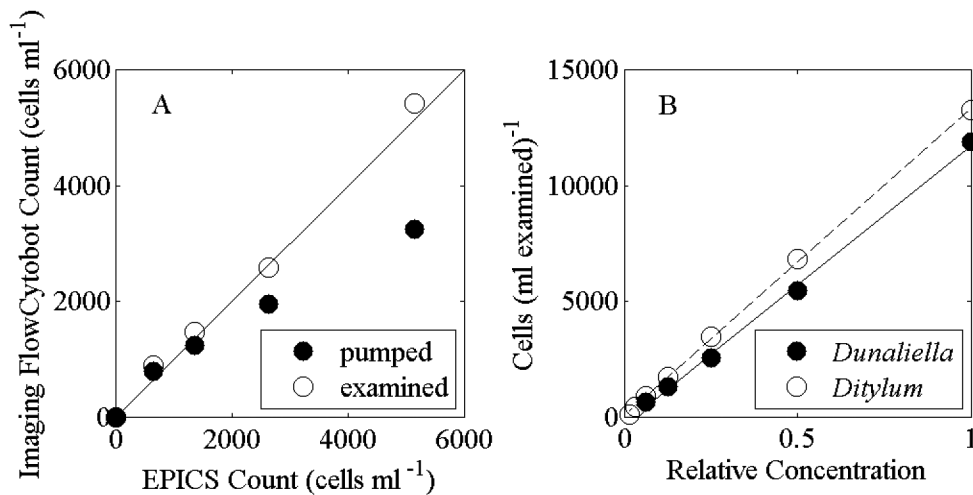


**Fig. 5.** Quantitation of cell counting. (A) Concentrations of 6- $\mu\text{m}$  *Dunaliella tertiolecta* cells measured with Imaging FlowCytobot were compared with those measured with a Coulter EPICS flow cytometer modified for high flow rate. “Electronic dead time” during image capture and analysis caused progressive undersampling as cell concentration increased (filled symbols), but by normalizing counts to the time actually spent examining sample water (open symbols), counts indistinguishable from those of the EPICS were obtained (see 1:1 line). (B) Results of dilution series for *Dunaliella* and for the much larger ( $\sim 20$  by  $100\ \mu\text{m}$ ) diatom *Ditylum brightwellii* are linear, indicating that cell concentrations measured by Imaging FlowCytobot are accurate to  $>10^4$  cells  $\text{mL}^{-1}$ .

A multifunction analog-digital board (104-AIO16-16E, Access I/O Products, Inc.) digitizes the integrated laser-derived signals and the duration of the triggering signals, produces analog signals to control the PMT high voltages, and carries out digital I/O tasks (e.g., motor control for focusing the objective and communication between software and hardware, i.e., inhibiting new trigger signals while the current image is being processed).

**Data analysis**—To minimize the resources needed for image data storage, Imaging FlowCytobot utilizes a “blob analysis” routine (Matrox Imaging Library 7.5) based on edge detection (changes in intensity across the frame) to identify regions of interest in each image. The subsampled images are transferred to a remote computer for storage and further analysis. For taxonomic classification, we developed an approach based on a support vector machine framework and several different feature extraction techniques; this approach is described elsewhere (Sosik and Olson 2007), along with results of automated classification of  $1.5 \times 10^6$  images obtained during Imaging FlowCytobot’s test deployment in Woods Hole Harbor.

For each particle, 5 channels of flow cytometric signal data are stored (integrated signals from fluorescence and light scattering detectors at 2 gain settings each, plus signal duration), along with a time stamp (10-ms resolution). Accumulated images and fluorescence/light scattering data are automatically transferred to the laboratory in Woods Hole every 30 min. The data are analyzed using software written in MATLAB (The Mathworks, Inc.).

**Deployment**—Imaging FlowCytobot is currently deployed by divers, who bolt the neutrally buoyant 70-kg instrument to a mounting frame located at 4-m depth on the MVCO Air Sea Interaction Tower (<http://www.whoi.edu/mvco>), and connect the power and communications cable, which is equipped with an underwater pluggable connector (Impulse Enterprise, Inc.).

Imaging FlowCytobot has been deployed at MVCO since 27 September 2006.

### Assessment

**Cell quantitation**—Hydrodynamic focusing causes all the cells in a sample to pass through Imaging FlowCytobot’s analysis region, so cell concentrations can be calculated, to a first approximation, by dividing the number of triggers by the volume of water analyzed (as determined by the analysis time and the known rate of flow from the syringe pump). However, this concentration is an underestimate, because during the time required to acquire and process each image, sample continues to flow through the flow cell but no new triggers are allowed. The minimum time required by the camera for image acquisition is 34 ms (i.e., 30 frames  $\text{s}^{-1}$ ), but we determined empirically that with image processing to locate and store the region of interest, at least 86 ms was required by the system; very large cells required even more time. We therefore measure the image processing period for each cell using a software timer. By subtracting the sum of these periods from the total elapsed time, we determine how much time is actually spent “looking” for cells, and use this value to calculate cell concentration in each syringe sample.

To evaluate cell quantitation by Imaging FlowCytobot, we analyzed replicate samples with both Imaging FlowCytobot and a Coulter EPICS flow cytometer, a nonimaging instrument capable of measuring cells at rates  $>10^3\ \text{s}^{-1}$ . We used a laboratory culture of *Dunaliella tertiolecta*, a small (6  $\mu\text{m}$ ) phytoplankter, because cells in this size range can be reliably analyzed by both instruments. Using the measured analysis time as described above, Imaging FlowCytobot-derived cell concentrations were indistinguishable from those of the EPICS flow cytometer (Fig. 5A).

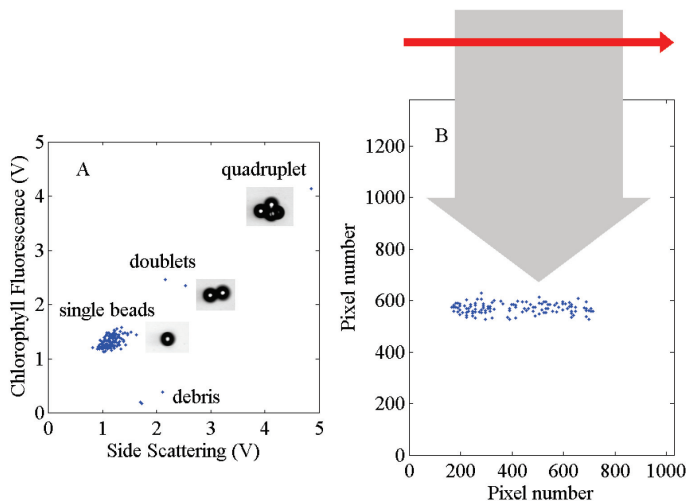


**Fig. 6.** Analysis of uniform fluorescent beads (20  $\mu\text{m}$ , Duke Scientific) illustrates Imaging FlowCytobot's measurements of fluorescence and scattering; single beads are easily distinguished from doublets and clumps of beads (A). This precision is the result of hydrodynamic focusing of the sample stream, which confines sample particles to the central core of the flow cell; the core can be visualized (B) by plotting the position of each bead's image in the camera's field of view. The flow (gray arrow) is downward at 2.2  $\text{m s}^{-1}$  and imaging takes place 270  $\mu\text{s}$  after a particle passes through the laser beam (red arrow). An image from each population is shown.

Analyses of dilution series of *Dunaliella* and of a much larger diatom (*Ditylum brightwellii*,  $\sim 20$  by 100  $\mu\text{m}$ ), which often required additional time ( $>86$  ms) for image processing, indicated that cell concentrations from Imaging FlowCytobot were reliable for both sizes of cells, up to at least  $1.5 \times 10^4$  cell  $\text{mL}^{-1}$  (Fig. 5B), very high concentrations for marine nanoplankton.

**Standard beads to assess flow cytometric measurements**—Measurements of uniform beads indicate that light scattering and fluorescence data are quantitative (Fig. 6); signals are uniform across the 150  $\mu\text{m}$ -wide sample core, and the coefficient of variation of bead fluorescence signals is typically  $<10\%$  even after extended periods of deployment. Although the flow cytometric measurements are probably of less interest than the images of cells, it is important to note that the acquisition of each image is initiated by the detection of a signal exceeding a threshold, so it is important to monitor detection efficiency during operation.

**Phytoplankton populations**—Analysis of seawater samples by Imaging FlowCytobot illustrates some advantages of the approach over conventional flow cytometry and manual microscopic analyses. First, flow cytometric sorting of particles in seawater has shown that light scattering/fluorescence signatures are rarely sufficient to identify nano- or microplankton at the genus or species level. Discrete populations are rarely discernible in a plot of light scattering vs. fluorescence (e.g., Fig. 7), and even if they are, it is difficult to be sure of their identity without cell sorting and examination. The images associated with the flow cytometric data reinforce this idea—different species do have characteristic light scattering/

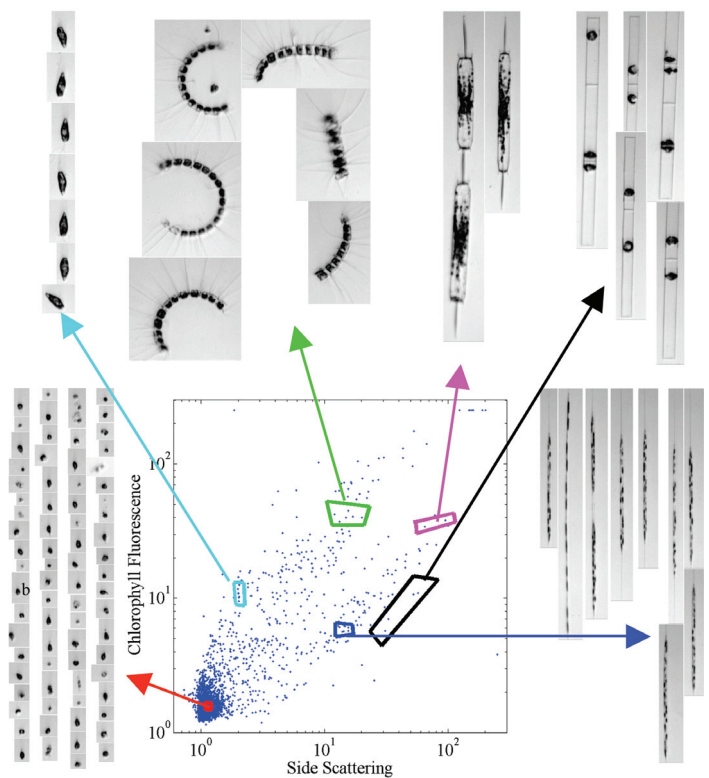


**Fig. 7.** Flow cytometric measurements of side scattering and chlorophyll fluorescence, and selected images of phytoplankton cells in a seawater sample from Woods Hole Harbor (Dec. 2004), analyzed by Imaging FlowCytobot (triggered by chlorophyll fluorescence). All images are shown at the same scale; the smallest cells are  $\sim 5$   $\mu\text{m}$ . Different regions in the scattering/fluorescence signature contain different species, but population boundaries are indistinct. Cell images (clockwise from lower left): mixed "small cells," *Euglena* spp., *Chaetoceros* spp., *Ditylum* spp., *Dactyliosolen* spp., *Rhizosolenia* spp.

fluorescence signatures, but these generally form a continuum (and often overlap) and so are not very useful in determining species composition. (The homogeneous populations of cells indicated by the image groupings in Fig. 7 are not random selections, but were obtained by trial-and-error searches of small regions of the plot; other regions show mixtures of species.) Thus, imaging allows us to greatly improve the accuracy of identification of different cells.

Imaging can also be used to study nonphytoplankton particles (Fig. 8), whose composition and abundance patterns are almost unknown. Triggering from light scattering rather than fluorescence signals reveals that the large majority of the particles in this seawater sample were not phytoplankton, but included various forms of detritus, empty diatom frustules, and heterotrophic organisms.

Preliminary comparisons of Imaging FlowCytobot's performance to traditional manual microscopy are encouraging (Fig. 9). For the dominant and most easily recognized cells in the water sample (the diatom *Guinardia* spp.), the counts were

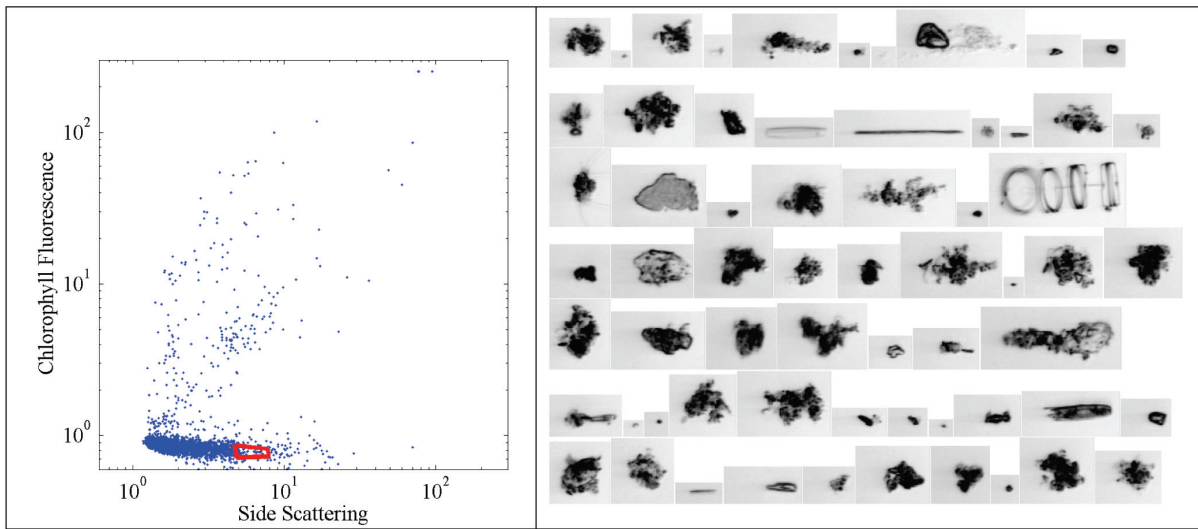


**Fig. 8.** As for Fig. 7, but triggered by light scattering. Note the large number of detritus particles (including empty diatom frustules) relative to chlorophyll-containing cells.

very close. For some categories, such as dinoflagellates, Imaging FlowCytobot counts were lower, probably because the distinguishing features of dinoflagellate cells (e.g., cingulum) were not always visible in the images (due to orientation) or were insufficiently resolved. Dinoflagellates are often highly pigmented relative to other cells of interest, so the illumination conditions used in Imaging FlowCytobot caused the cells to appear very dark (even though green illumination, which is not strongly absorbed by photosynthetic pigments, was used to minimize this effect). It is likely that many dinoflagellates were classified as “round 20 μm cells,” of which Imaging FlowCytobot saw many more than the microscopist. For almost all of the more rare categories, Imaging FlowCytobot found more cells than microscopy, sometimes many more. Sometimes this was because the plankton groups were not counted by the kind of microscopy/sample preservation method used (ciliates, small dinoflagellates, flagellates), but others remain unexplained (*Cylindrotheca*, *Licmophora*, pennate diatoms).

A second strength of Imaging FlowCytobot is the greatly increased scope made possible by the automated nature of the approach. A test deployment of Imaging FlowCytobot at 5 m depth off the WHOI pier (Fig. 10) showed that the instrument is capable of operating without external maintenance for at least 2 months. The results presented here are simply cell counts, showing long-term trends in cell abundance, with superimposed higher-frequency periodicity (probably tidal). Analyzing seawater at a nominal rate of 0.25 mL min<sup>-1</sup>, more than 1.5 million images were collected during this deployment; the analysis of these images with an automated approach is presented in a companion paper (Sosik and Olson 2007).

*Image quality*—The ultimate resolution of the optical system is determined by the 10× microscope objective, which has a theoretical resolution of ~1 μm. As presently configured, a

20-μm bead spans 68 pixels (3.4 pixels/μm), so the camera resolution is more than adequate for this objective. However, image quality will be affected by several additional factors in Imaging FlowCytobot, including cell motion, flash lamp pulse duration, and location of cells in the flow cell.

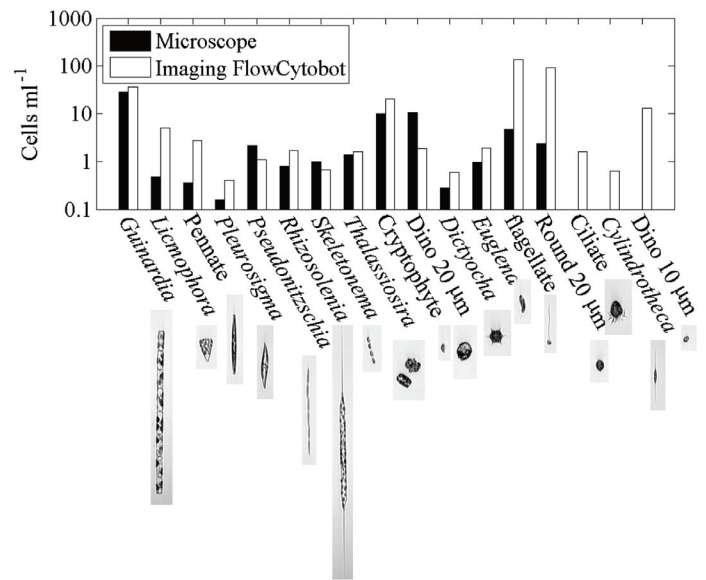


**Fig. 9.** Microplankton community composition in a surface seawater sample from Woods Hole Harbor (9 February 2006), as analyzed by Imaging FlowCytobot and by manual microscopy. The sample was split and 100 mL was fixed with Lugol’s solution and settled in an Utermohl chamber for examination by a trained taxonomist. The same sample volume was analyzed by Imaging FlowCytobot, with subsequent manual image classification. Only categories with 10 or more observations are shown. Numbers of chain-forming cells were estimated as described in “Comments and Recommendations.”

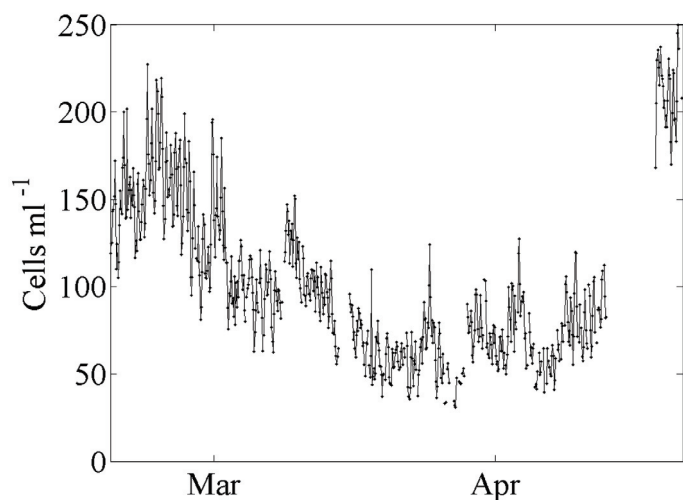


**Fig. 10.** Phytoplankton cell concentrations measured by Imaging FlowCytobot during test deployment in Woods Hole Harbor in 2005.

Movement of the subject due to sheath flow during the camera exposure will tend to blur the image in the direction of flow. Sample particle velocity was determined (by measuring the image displacement caused by a known change in strobe delay) to be  $2.2 \text{ m s}^{-1}$ , so the subject moves 7.5 pixels during the  $1\text{-}\mu\text{s}$  exposure. The effect of this movement is visible in an image of a plastic bead as a thickening of the leading and trailing edges, relative to the upper and lower edges (not shown). In addition, although most of the light energy from the xenon flash is emitted within  $1 \mu\text{s}$ , the flash decays over several microseconds, which produces a “shadow” downstream of high-contrast subjects. These factors limit the velocity of flow that can be employed, and thus the sampling rate of the instrument (although a shorter flash, as from an LED or pulsed laser, could be used to address this limitation).

The sample core in Imaging FlowCytobot is about  $150 \mu\text{m}$  wide (see Fig. 6B), so if we assume that the core has the same shape as the channel, the thickness of the core would be  $\sim 33 \mu\text{m}$ . This is somewhat greater than the theoretical depth of focus of a  $10\times$  objective with N.A. 0.2 ( $\sim 10 \mu\text{m}$ ). As the thickness of the sample core increases, more particles will be out of focus, which will limit both the sampling rate and the optical resolution that can be employed. Finally, the illumination conditions (e.g., condenser aperture, which is dictated by the amount of light available during the flash) affect the resolution and contrast of the image.

## Discussion

Plankton in the size range  $10$  to  $100 \mu\text{m}$ , which includes many diatoms and dinoflagellates, are critical components of coastal ecosystems, but their regulation is relatively poorly understood because it is difficult to sample them adequately in the dynamic coastal environment. An important part of this sampling problem is now addressed by Imaging FlowCytobot's

unprecedented capabilities for autonomously obtaining quantitative data on nano- and microphytoplankton, with images of sufficient quality to allow taxonomic resolution to genus or even species level in some cases, high sampling resolution (typically,  $5 \text{ mL}$  seawater analyzed every  $20 \text{ min}$ ), and long endurance (months). These capabilities, in combination with the automated image classification approach described in the companion paper (Sosik and Olson 2007), will allow oceanographers to carry out a wide variety of studies of species succession, responses of communities to environmental changes, and bloom dynamics with vastly improved resolution and scope. These improvements promise to lead to improved understanding of many aspects of plankton ecology.

## Comments and Recommendations

*Limitations on deployment duration*—The limiting factor for Imaging FlowCytobot's endurance in the field appears to be wear of the syringe plunger seal, which eventually leaks water into the housing. This is also the case with FlowCytobot, and could conceivably be prevented by advances in materials used for the seal. The problem is exacerbated by low temperatures, as the syringe is designed for use at room temperature (Kloehn, Inc., personal communication) and the seal shrinks significantly as temperatures approach freezing. Even so, FlowCytobot has had a successful 6-month deployment, and Imaging FlowCytobot's successful 2-month test deployment included periods with water temperatures approaching  $0^\circ\text{C}$ . We have taken the precaution of installing temperature and humidity sensors inside the housing, which provides warning of slow leaks due to syringe wear. Before closing, the housing is flushed with dry nitrogen and a packet of silica gel desiccant is placed inside, to prevent condensation. As a precaution against internal leaks in the tubing or flow cell, the sample inlet and overflow ports are fitted with solenoid valves (Reet Corp.) that close if humidity rises above a preset level (or if power is interrupted). To help analyze potential problems, we store temperature and humidity data along with each image, so we can monitor the history of conditions inside the instrument.

*Beads as internal standards*—The acquisition of each image is initiated by the detection of a fluorescence (or scattering) signal exceeding a threshold, so it is important to monitor detection efficiency during operation. In the original FlowCytobot, this is accomplished using periodic automated sampling of  $1\text{-}\mu\text{m}$  beads. For Imaging FlowCytobot, we need to use beads that are much larger and whose fluorescence is excited by red light, and these have proved more difficult to use as internal standards. During the 2-month test deployment of Fig. 10, suitable standard beads were not available, but since then we have obtained red-excited beads of  $9\text{-}$  and  $20\text{-}\mu\text{m}$  diameter, which are now periodically analyzed as part of the sampling program. Initially, the number of beads sampled decreased dramatically after only a few days' deployment, probably because the relatively large size of these beads causes them to sink rapidly, and because the beads can stick to the walls of the

reservoir and/or tubing. Using a magnetic stirrer to mix the suspension of beads before each sampling, and adding bovine serum albumin and detergent to reduce stickiness (Velikov et al. 1998), has reduced the loss of beads over time, but we are still working on this problem.

*Quantifying chain-forming cells*—Chain-forming diatoms, which often dominate coastal blooms, present a special counting problem. Ideally, we want to know the number of cells present, not simply the number of chains (which can vary widely in length). For the comparison between microscopic counts and Imaging FlowCytobot results (Fig. 9), therefore, we manually counted each cell in images of the chain-forming diatoms (*Guinardia*, *Thalassiosira*, *Nitzschia*, *Skeletonema*, and *Thalassionema*). We also used the measured duration of the chlorophyll fluorescence signal for each chain, calibrated by manual counts of the cells in each chain, to estimate cell numbers. This approach allows us to estimate the number of cells in chains that extend out of the camera's field of view (those more than  $\sim 300\ \mu\text{m}$ ), by extrapolating the relationship between cells per chain and signal duration. For the seawater sample in Fig. 9, for example, *Guinardia* chains of up to 32 cells were observed by microscopy, whereas the maximum number of cells visible in Imaging FlowCytobot images was 13; correction for these "unimaged" cells increased the Imaging FlowCytobot estimate of *Guinardia* cells from 607 to 920.

This approach requires manual calibration for each chain-forming species (although we plan to investigate automated image analysis for this task) and will be affected by changes in the size of the individual cells. In addition, the timing of the flash lamp limits signal durations to  $\sim 270\ \mu\text{s}$ , so cell numbers for chains longer than  $600\ \mu\text{m}$  will be minimum estimates.

## References

- Austin, T., and others. 2002. A network-based telemetry architecture developed for the Martha's Vineyard coastal observatory. *IEEE J. Oceanic Eng.* 27: 228-234.
- . 2000. The Martha's Vineyard Coastal Observatory: A long-term facility for monitoring air-sea processes. *Proc. Oceans 2000* 3: 1937-1941.
- Cunningham, A., D. McKee, S. Craig, G. Tarran, and C. Widdicombe. 2003. Fine-scale variability in phytoplankton community structure and inherent optical properties measured from an autonomous underwater vehicle. *J. Mar. Sys.* 43: 51-59.
- Daly, K. L., R. H. Byrne, A. G. Dickson, S. M. Gallager, M. J. Perry, and M. K. Tivey. 2004. Chemical and biological sensors for time-series research: Current status and new directions. Marine Technology Society.
- Jahnke, R. and others. 2004. Coastal Observatory Research Arrays: A Framework for Implementation Planning. Report on the CoOP CORA Workshop. Skidaway Institute of Oceanography Technical Report Draft TR-03-01, 69.
- Olson, R. J., A. A. Shalapyonok, and H. M. Sosik. 2003. An automated submersible flow cytometer for pico- and nanophytoplankton: FlowCytobot. *Deep-Sea Res. I* 50: 301-315.
- SCOTS Steering Committee. 2002. SCOTS: Scientific cabled observatories for time series, Workshop report, <http://www.coreocean.org/SCOTS/>. 88.
- Sieracki, C. K., M. E. Sieracki, and C. S. Yentsch. 1998. An imaging-in-flow system for automated analysis of marine microplankton. *Mar. Ecol. Prog. Ser.* 168: 285-296.
- Sosik, H. M., and R. J. Olson. 2007. Automated taxonomic classification of phytoplankton sampled with image-in-flow cytometry. *Limnol. Oceanogr. Methods* in press.
- , R. J. Olson, M. G. Neubert, A. A. Shalapyonok, and A. R. Solow. 2003. Growth rates of coastal phytoplankton from time-series measurements with a submersible flow cytometer. *Limnol. Oceanogr.* 48: 1756-1765.
- Thwaites, F. T., S. M. Gallager, C. S. Davis, A. M. Bradley, A. Girard, and W. Paul. 1998. A winch and cable for the autonomous vertically profiling plankton observatory. *Oceans 98 - Engineering for sustainable use of the oceans: conference proceedings 28 September - 1 October 1998* 1: 32-36.
- Velikov, K. P., F. Durst, and O. D. Velev. 1998. Direct observation of the dynamics of latex particles confined inside thinning water-air films. *Langmuir* 14: 1148-1155.

Submitted 5 October 2006

Accepted 27 February 2007